ACS APPLIED MATERIALS & INTERFACES

Letter

www.acsami.org

Efficient Luminescence from Perovskite Quantum Dot Solids

Younghoon Kim,[†] Emre Yassitepe,[†,‡] Oleksandr Voznyy,[†] Riccardo Comin,[†] Grant Walters,[†] Xiwen Gong,[†] Pongsakorn Kanjanaboos,[†,#] Ana F. Nogueira,[‡] and Edward H. Sargent*[,†]

[†]Department of Electrical and Computer Engineering, University of Toronto, 10 Kings College Road Toronto, Ontario M5S 3G4, Canada

[‡]Institute of Chemistry, University of Campinas, UNICAMP, P.O. Box 6154, 13084-971 Campinas, São Paulo, Brazil

Supporting Information

ABSTRACT: Nanocrystals of $CsPbX_3$ perovskites are promising materials for light-emitting optoelectronics because of their colloidal stability, optically tunable bandgap, bright photoluminescence, and excellent photoluminescence quantum yield. Despite their promise, nanocrystal-only films of $CsPbX_3$ perovskites have not yet been fabricated; instead, highly insulating polymers have been relied upon to compensate for nanocrystals' unstable surfaces. We develop solution chemistry that enables single-step casting of perovskite nanocrystal films and overcomes problems in both perovskite quantum dot purification and film fabrication. Centrifugally cast films retain bright photoluminescence and achieve dense and homogeneous morphologies. The new materials offer a platform for optoelectronic applications of perovskite quantum dot solids.

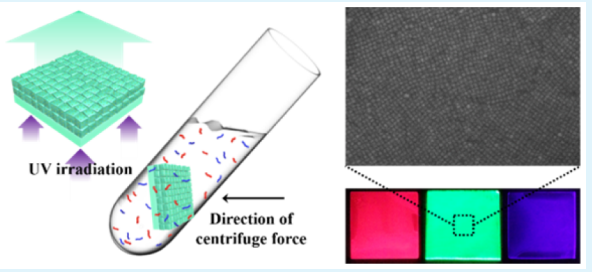

KEYWORDS: *cesium lead halide, perovskites, quantum dots, centrifugal casting, nanocrystal films*

Semiconducting metal halide perovskites have attracted considerable attention in optoelectronics, including photovoltaics and light emission, because of their excellent photophysical properties.[1−9] Perovskite-based photovoltaic devices showing power conversion efficiency exceeding 20% have been recently reported,[4] whereas perovskite-based films and light-emitting devices show quantum efficiencies in the range 0.1−3.5%, indicating opportunities for further improvement.[5−9]

The photoluminescence of lead halide perovskites can be improved through dimensional control via nanostructuring and judicious surface passivation.[10,11] Thanks to recent advances in nanomaterials synthesis, $CsPbX_3$ (X = Cl, Br, and I) perovskite-based colloidal nanocrystals, hereafter referred to as perovskite quantum dots, have recently been constructed and investigated by several research groups. These materials have excellent photophysical properties including narrow emission line width, high quantum yield of luminescence, and short radiative lifetimes.[12−18] These improved photophysical properties were attributed to nanoscale effects such as quantum confinement.

Protesescu et al. recently reported fully inorganic $CsPbX_3$ perovskites prepared in the form of colloidal nanocrystals. These employed hydrophobic ligands and were dispersed in nonpolar solvents.[13,14] Next-generation nanoscale $CsPbX_3$ perovskites have also been developed.[16,17] Attractively, the bandgap is readily controlled in $CsPbX_3$ in view of its larger exciton Bohr diameter, estimated to be of order ∼12 nm.

To date, the most monodispersed and crystalline perovskite quantum dots have relied on hydrophobic ligands for colloidal stabilization in nonpolar solvents.[13−20] To purify high-quality nanocrystals, i.e., to remove remnant precursors, polar solvents are added, and these serve as an antisolvent, after which the resultant mixture is centrifuged.

Unfortunately, the underlying perovskite crystal materials are unstable (prone to dissolution) in polar solvents.[13,21] For this reason, it is necessary to minimize the purification steps that would normally rely on addition of an antisolvent followed by centrifugation. This complicates the formation of films based on perovskite nanocrystals, especially when it is desired to preserve the high luminescence of the input colloidal materials. Traditional means of film formation such as spin-coating normally rely on well-purified nanocrystal solutions that are not currently available in the case of perovskite quantum dots.

For this reason, the realization of purified perovskite quantum dot films has remained elusive. Perovskite nanocrystal/polymer composite thick pellets have been fabricated by embedding the nanocrystals in an insulating poly(methylmetacrylate) (PMMA) matrix;[13,15] however, optoelectronic applications such as light-emitting diodes (LEDs) rely on pure films of nanocrystals that do not include an insulating phase, and also require effective removal of synthetic precursors.

We took the view that, to avoid damage from crystal-destabilizing polar solvents, a procedure to form perovskite quantum dot films could instead be developed that would involve a centrifugation-based process applied directly to

Received: September 25, 2015
Accepted: November 3, 2015

DOI: 10.1021/acsami.5b09084
ACS Appl. Mater. Interfaces XXXX, XXX, XXX−XXX

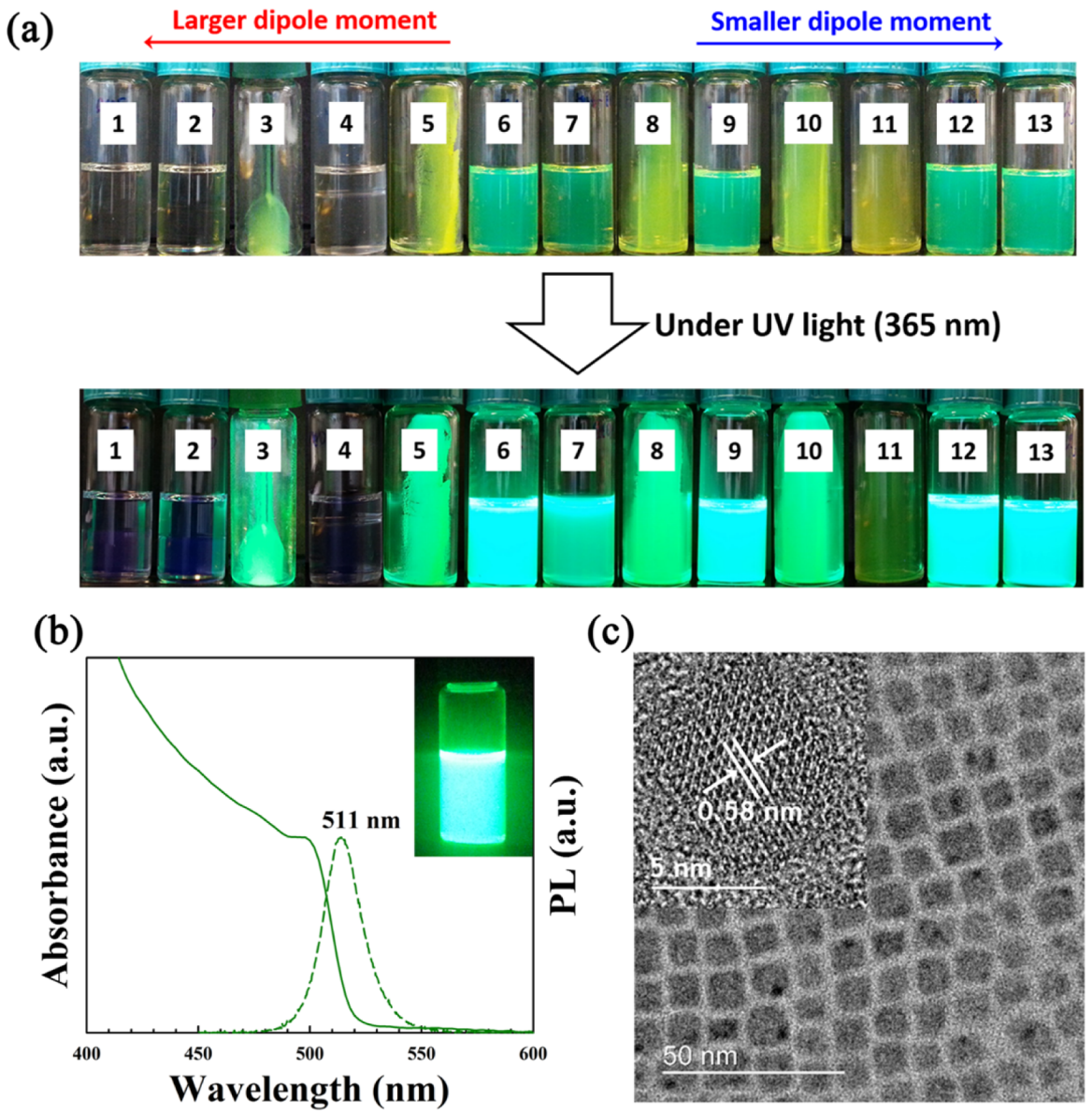

Figure 1. (a) Effect of polar solvents on crude solutions of as-synthesized $CsPbBr_3$ nanocrystals. All mixtures of crude solution and polar solvents (with the volume ratio of one to one) in each vial were centrifuged at 8000 rpm for 30 min. The solvents are arranged in order of increasing dipole moment: (1) dimethyl sulfoxide, (2) dimethylformamide, (3) acetonitrile, (4) methanol, (5) acetone, (6) ethyl acetate, (7) tert-butanol, (8) 1-butanol, (9) tetrahydrofuran, (10) isopropyl alcohol, (11) ethanol, (12) chloroform, and (13) dichloromethane, respectively. (b) UV−vis absorbance and PL spectra of the once-purified $CsPbBr_3$ nanocrystal solution redispersed in hexane. The inset features the stable and bright luminescence $CsPbBr_3$ nanocrystals. (c) HR-TEM image of $CsPbBr_3$ nanocrystals with the diameter of approximately 7 nm.

colloids, leading to the formation of on a substrate.[22−25] This would also provide an added means of purification of the dots relative to the precursors, since it was expected that the nanocrystals would deposit but leave remaining precursors still solubilized in the supernatant. In recent related reports, PbS colloidal quantum dot solids based on chalcogenides were fabricated using centrifugal colloidal casting; however, this approach relied on an exchange to short polar ligands for deposition from a polar solvent.[26] It was not possible to translate this approach directly to nanocrystals of $CsPbX_3$ perovskites in light of their unstable surfaces in polar solvents. We would need to develop a protocol that would instead minimize the use of polar solvent.

Here we report the first highly luminescent solids made using perovskite quantum dots; we achieve this via a new process, the direct single-step centrifugal casting of $CsPbBr_3$ nanocrystals. We deposited films from crude solution of as-synthesized $CsPbBr_3$ nanocrystals with only small addition of a weakly polar solvent. We found that these centrifugally cast films show bright luminescence with dense and homogeneous morphologies; and achieve significant purification with the minimal use of destabilizing polar antisolvents. This provides a major advance over spin-coating to produce perovskite quantum-tuned films. We also show the versatility in the centrifugal process, proving its application to $CsPbI_3$ and $CsPbCl_3$ perovskite nanocrystals.

Bright solutions of as-synthesized $CsPbBr_3$ nanocrystals in a nonpolar solvent (i.e., hexane, octane, and toluene) exhibited characteristic absorbance and emission peaks resulting from localization. To remove precursors, we centrifuged the solutions a single time following the addition of an antisolvent

DOI: 10.1021/acsami.5b09084
ACS Appl. Mater. Interfaces XXXX, XXX, XXX−XXX

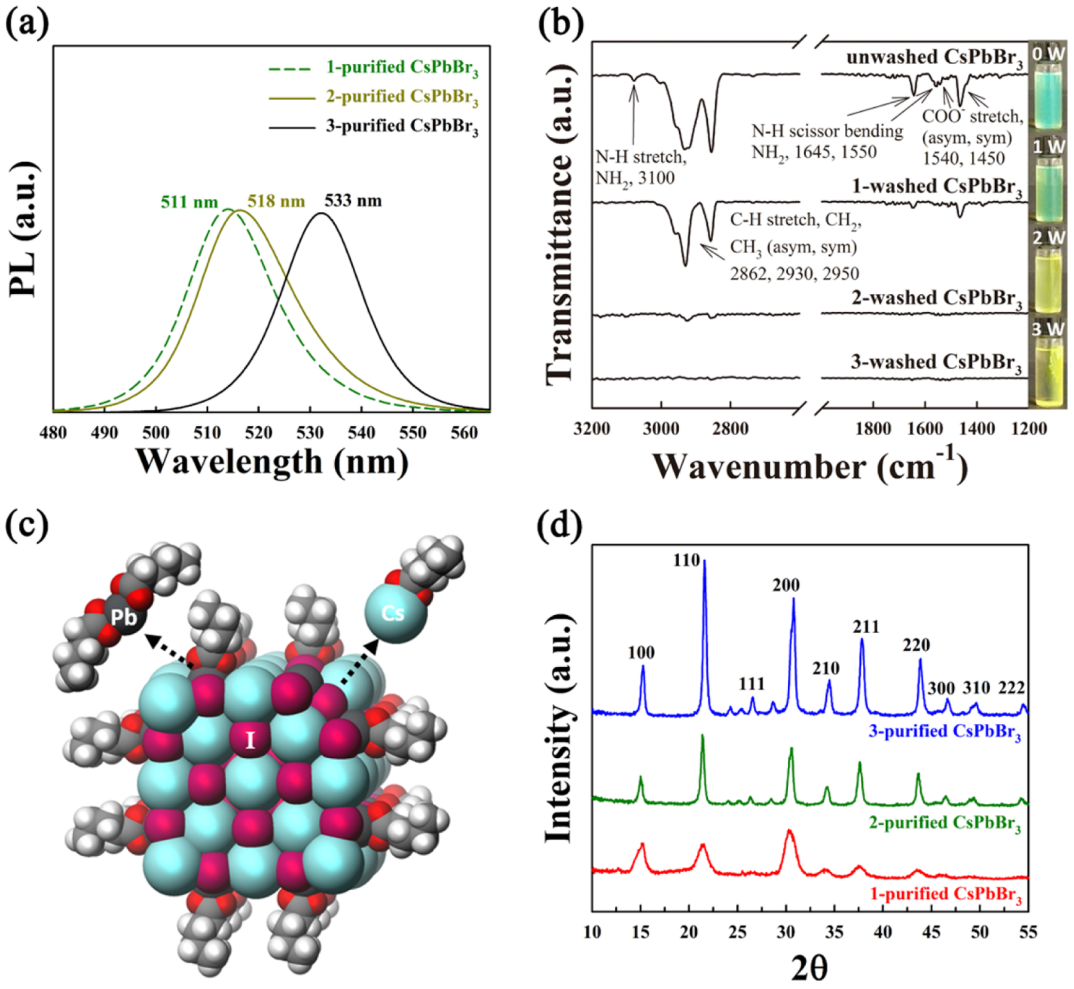

Figure 2. (a) PL spectra of 1-, 2-, and 3-purified $CsPbBr_3$ nanocrystal solutions. (b) FTIR spectra and photo images of $CsPbBr_3$ perovskites as a function of the purification steps. (c) DFT simulations of $CsPbX_3$ perovskites showing the weak binding strength of the surface ligands. (d) Powder XRD pattern of the $CsPbBr_3$ perovskites according to the number of purification steps.

and then redispersed in hexane. To separate $CsPbBr_3$ nanocrystals from the crude solution, it is important to introduce the polar solvent at very low concentrations as an antisolvent. In contrast with chalcogenide quantum dots, lead halide perovskites are not stable in many common solvents, and in particular in polar solvents, a consequence of the fact that they are fully ionic crystals.[13,21] We posited that it would be necessary to select a polar solvent that enables precipitating the nanocrystals by centrifugation while minimizing the corresponding damage to the nanocrystal surfaces.

We first investigated polar solvent effects on the as-synthesized $CsPbBr_3$ nanocrystals. For this investigation, all mixtures of crude solution and each polar solvent (with the volume ratio of one to one) were centrifuged at 8000 rpm for over 30 min. The results indicate that from mildly polar solvents, isopropyl alcohol, 1-butanol, acetone, and acetonitrile enabled complete precipitation of $CsPbBr_3$ nanocrystals via centrifugation (Figure 1a). We selected isopropyl alcohol as antisolvent in our experiments since it possesses the smallest dipole moment (~1.66 D). We also studied the impact of antisolvent concentration. $CsPbBr_3$ nanocrystals in crude solution were precipitated when centrifuged in the presence of antisolvent when the volume ratio antisolvent:original solution exceeded 1:1. Much larger excess quantities resulted in the dissolution of particles (Figure S1). The amount of antisolvent needed to be carefully calibrated and controlled when purifying the $CsPbX_3$ nanocrystals using centrifugation.

Figure 1b shows that purified $CsPbBr_3$ nanocrystals that employed centrifugation with isopropyl alcohol as antisolvent exhibit highly stable and bright luminescence. They retain their optical properties and showed no appreciable change in absorbance and emission spectra compared to the as-synthesized solution-phase materials (Figure S2). High-resolution transmission electron microscopy (HR-TEM) indicates that 7 nm-diameter $CsPbBr_3$ nanocrystals were highly monodispersed, with a cubic shape and narrow size distribution after once purification step (Figure 1c). The inset in Figure 1c highlights that $CsPbBr_3$ nanocrystals possess a well-defined crystalline structure with a cubic lattice parameter of 0.58 nm along the crystalline direction ⟨110⟩.

We attempted additional purification steps in order to acquire better-purified $CsPbBr_3$ nanocrystals; this resulted in the agglomeration and fusion of $CsPbBr_3$ nanocrystals due to the significant deterioration of colloidal stability of the nanocrystals. In addition, PL spectra were significantly red-shifted in comparison to Figure 1b, suggesting conversion to bulk $CsPbBr_3$ (Figure 2a and Figure S3).[27] We obtained Fourier transform infrared (FTIR) spectra of $CsPbBr_3$ nanocrystals across the various purification steps (Figure 2b). For the synthesis of $CsPbX_3$ nanocrystals, oleylamine (OLA) is

DOI: 10.1021/acsami.5b09084
ACS Appl. Mater. Interfaces XXXX, XXX, XXX−XXX

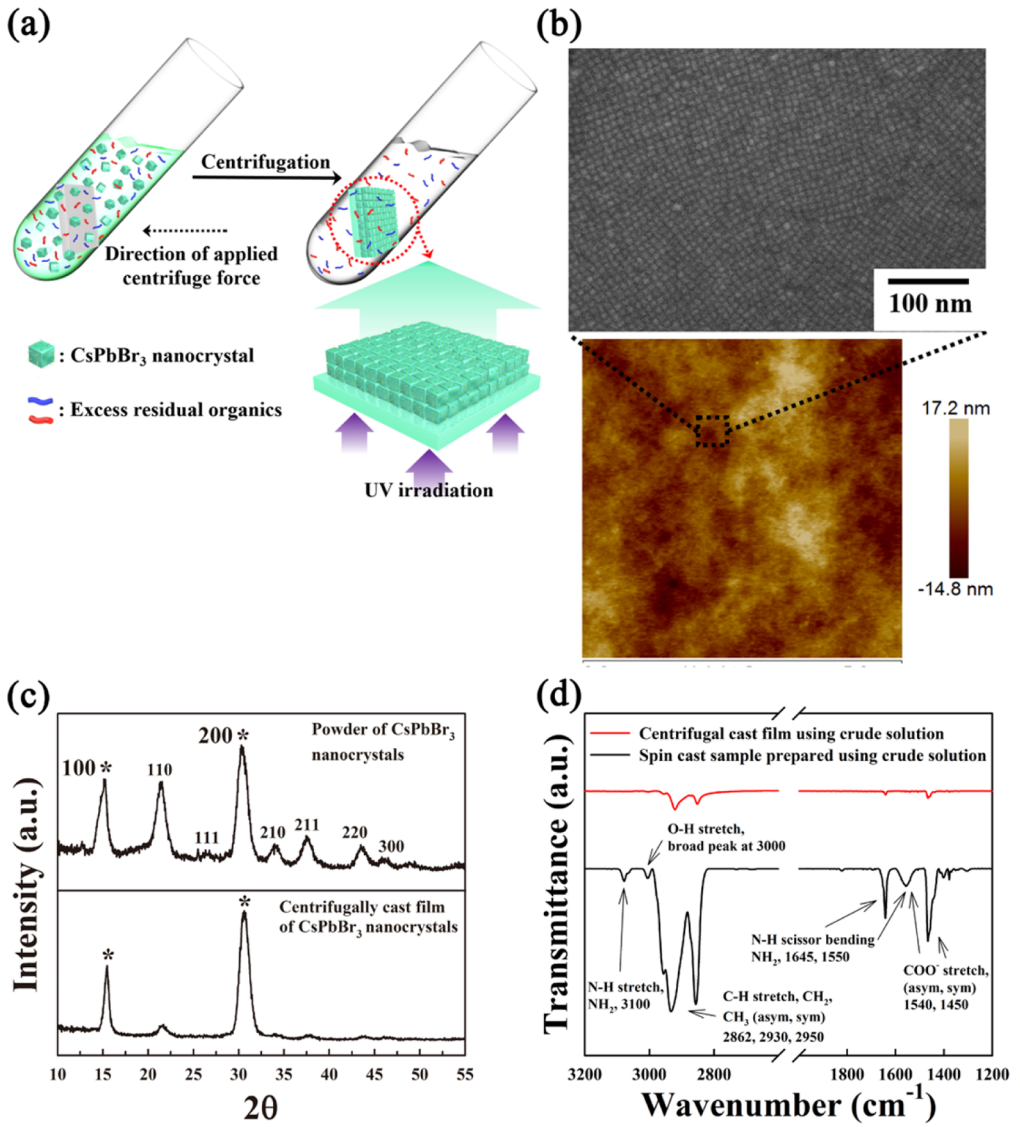

Figure 3. (a) Schematic illustration of the centrifugal casting process, which enables simultaneous purification and film fabrication using crude solutions of as-synthesized $CsPbX_3$ nanocrystals. (b) FE-SEM and AFM images for centrifugally cast film of $CsPbBr_3$ nanocrystals. (c) XRD pattern for powder and centrifugally cast film of $CsPbBr_3$ nanocrystals. (d) FTIR spectra of spin-cast (black) and centrifugally cast (red) films prepared from the crude solution of as-synthesized $CsPbBr_3$ nanocrystals, indicating that centrifugal casting process enabled the effective removal of excess residuals and passivation by the remaining ligands binding $CsPbBr_3$ nanocrystals.

responsible for solubilizing lead halide (PbX_2) salts in the octadecene (ODE) solvent, while oleic acid (OA) enables colloidal dispersion of the resulting nanocrystals in the nonpolar solvent (Experimental Section in the Supporting Information).[13] The crude solution of as-synthesized $CsPbBr_3$ nanocrystals (corresponding to the unpurified $CsPbBr_3$ of Figure 2b) showed an FTIR spectrum that revealed the presence of aliphatic hydrocarbon chains, amine ($-NH_2$), and carboxylic acid ($-COOH$) moieties, indicating that significant quantities of precursors (i.e., OLA, OA, and ODE) are retained in the crude solution. In particular, the carboxylate ($-COO^-$) stretching mode indicates that $-COOH$ groups of OA ligands are bound to the surface of $CsPbBr_3$ perovskites in the form of $-COO^-$ groups, consistent with the fact that the resulting $CsPbBr_3$ nanocrystals were observed to be colloidally dispersible in nonpolar solvents. Although these signals are significantly reduced after one purification step, the resulting $CsPbBr_3$ still retain a stable colloidal form in the nonpolar solvent, suggesting that $CsPbBr_3$ nanocrystals were stabilized by the remaining ligands. These FTIR signals completely disappeared upon further purifications; and complete purification invariably led to a complete loss of colloidal stability: the detachment of the ligands causes $CsPbBr_3$ nanocrystals to agglomerate and fuse, leading to the loss of quantum confinement.

Density functional theory (DFT) simulations confirm the weak binding strength of these ligands and clarify that it is easier to desorb ligands as neutral Cs-oleate or Pb-oleate species, with binding energies ~0.5 and ~1 eV, respectively, rather than as oleate itself, whose binding energy of ~2 eV is much higher (Figure 2c). More details of DFT simulations are provided in the Supporting Information. Nanocrystal fusion was also confirmed using powder X-ray diffraction (XRD), which showed gradually higher and sharper diffraction patterns with increasing numbers of purification steps (Figure 2d).

DOI: 10.1021/acsami.5b09084
ACS Appl. Mater. Interfaces XXXX, XXX, XXX−XXX

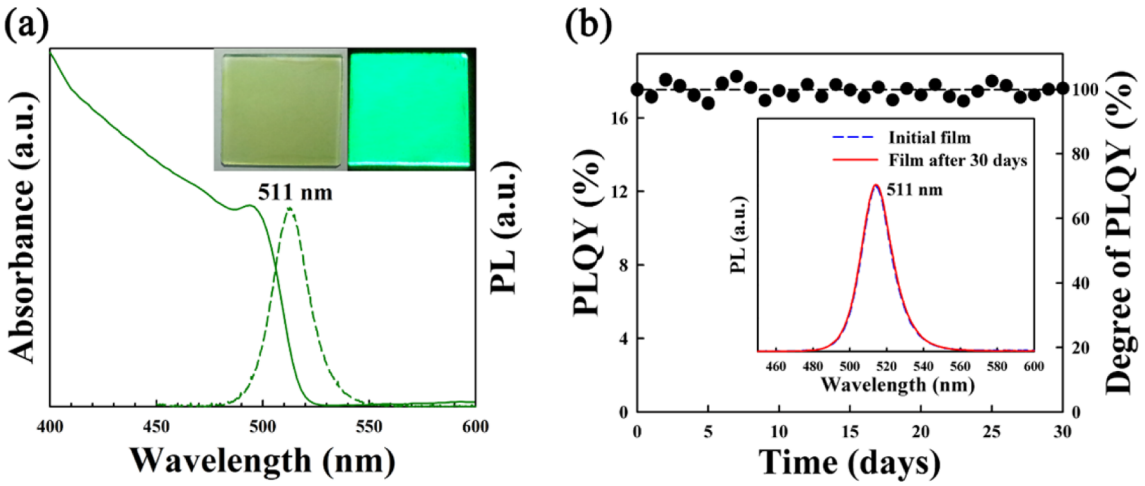

Figure 4. (a) UV−vis absorbance and PL spectra of centrifugally cast film of $CsPbBr_3$ nanocrystals. The photographic images in a show a $CsPbBr_3$ nanocrystal film fabricated onto a glass substrate. It sits in front of white paper and is UV photoexcited. (b) PLQY stabilities of centrifugally cast film of $CsPbBr_3$ nanocrystals stored under ambient conditions. The inset data indicate that the $CsPbBr_3$ nanocrystal-based films preserve their initial PL emission peak over the course of multiple weeks.

As a result, though one-time-purified $CsPbBr_3$ nanocrystals are stable, we were unable to fabricate compact and crack-free films using conventional spin- and/or dip-coating methods: residual chemicals in $CsPbBr_3$ nanocrystal led to poor morphology and evidence of separate organic-rich vs nanocrystal-rich phases (Figure S4). We also carried out additional centrifugation of the one-time-purified $CsPbBr_3$ nanocrystals using minimal amounts of antisolvent, sufficient to precipitate the $CsPbBr_3$ nanocrystals, in order to obtain more purified $CsPbBr_3$. Although we used minimal antisolvent to initiate precipitation of the one-time-purified $CsPbBr_3$ nanocrystals, even this very mild additional purification step resulted in a change in the PL emission peak (Figure S5).

Since our objective was to form $CsPbX_3$ nanocrystal-based films exhibiting a compact and crack-free morphology while preserving the inherent optical properties of the original $CsPbX_3$ nanocrystals, we sought to develop a centrifugal casting method for the formation of high-quality films of $CsPbBr_3$ nanocrystals. Our notion was to complete the purification procedure during deposition directly from the as-synthesized crude solution. For the film formation of $CsPbBr_3$ nanocrystals, the concentration of crude solution was adjusted to 1 mg mL^{-1} using hexane solvent. We placed the glass substrate in a centrifuge tube, adding the $CsPbBr_3$ nanocrystal solution into the tube with antisolvent (with volume ratio of one to one), and centrifuged the sample at 8000 rpm for 30 min. The $CsPbBr_3$ nanocrystals became physically adsorbed on the inserted glass substrate, a consequence of centripetal acceleration, and the resulting film-coated substrate was removed from the tube and dried to remove residual supernatant (Figure 3a).

As a result, we find that, only by developing this new variant of the centrifugal casting method, were we able to achieve simultaneous purification and formation of $CsPbBr_3$ nanocrystal films (Experimental Section in the Supporting Information). We systematically controlled film thickness by employing different concentrations of $CsPbBr_3$ once hexane solvent was added to as-synthesized $CsPbBr_3$ nanocrystal solutions (Figure S6).

The resulting $CsPbBr_3$ films showed dense packing and periodic nanocrystal assemblies, as well as compact crack-free morphologies (Figure 3b). Additionally, the surface morphologies of $CsPbBr_3$ films were obtained via scanning electron microscopy (SEM) over a range of regions of the sample (Figure S7). Using XRD studies of centrifugally cast films, we found that $CsPbBr_3$ nanocrystals were assembled with preferential orientation of (100) and (200) planes coplanar with the substrate planes. We confirmed that $CsPbBr_3$ nanocrystals, prepared as powders, showed XRD patterns characteristic of random orientation (Figure 3c).[28] We also confirmed using FTIR measurement that the signal from the residual supernatant (i.e., solvent, excess oleic acid and oleylamine, etc.) was substantially eliminated from the centrifugally cast films of $CsPbBr_3$ nanocrystals compared to the as-synthesized crude solution. We also confirmed that the centrifugally cast $CsPbBr_3$ nanocrystals remained passivated by the remaining ligands (Figure 3d). This result indicates that the centrifugal casting process enabled the successful purification as well as film formation of $CsPbBr_3$ nanocrystals.

Highly luminescent $CsPbBr_3$ films were successfully fabricated via centrifugal casting: indeed they exhibit no change in absorbance and emission peaks compared with the $CsPbBr_3$ nanocrystal solution. We conclude that the $CsPbBr_3$ nanocrystals retained quantum confinement and did not aggregate during the casting process (Figure 4a). This process also enabled the fabrication of nanocrystal-based thin films exhibiting both red and blue emission using $CsPbI_3$ and $CsPbCl_3$ perovskite nanocrystals (Figure S8). In particular, $CsPbI_3$ nanocrystals have a metastable structure because of their cubic phase transition at high temperature. However, our process enabled the fabrication of highly luminescent $CsPbI_3$ films that preserved the absorbance and emission peak of $CsPbI_3$ nanocrystals in solution phase. These films, too, exhibited preferential orientation assembly (Figure S9). We also successfully fabricated centrifugally cast films of mixed-halide $CsPb(I/Br)_3$ nanocrystals that also showed a single emission peak (Figure S10).

We then investigated the photoluminescence quantum yield (PLQY) of centrifugally cast films of $CsPbBr_3$ nanocrystals. The best films achieved PLQYs of 18%. This represents the first report, to our knowledge, of the PLQY of lead halide perovskite pure nanocrystal-based films. The measured PLQY of films was

DOI: 10.1021/acsami.5b09084
ACS Appl. Mater. Interfaces XXXX, XXX, XXX−XXX

about 3 times lower than in the solution phase in hexane (56%), a common phenomenon in colloidal quantum dot films.[29] In addition to being efficient in their PLQY, the films showed stability in their optical emission, with no change in the PL emission peak (~511 nm) over several weeks under ambient conditions (Figure 4b). This result is consistent with a highly stable film based on $CsPbBr_3$ nanocrystals that remain stabilized and passivated using their original ligands retained during the deposition process (Figure 3d). We also measured the PLQY of $CsPbI_3$ and $CsPbCl_3$ nanocrystals. The PLQY in solution (54%) and film (17%) of $CsPbI_3$ nanocrystals are similar to those of $CsPbBr_3$ nanocrystals. However, in case of $CsPbCl_3$ nanocrystals, which emit at short wavelength (~410 nm), the solution and film show lower PLQY values of 3 and 1%, respectively. Similar results have been obtained before in chloride perovskite films.[30]

These findings demonstrate that $CsPbX_3$ nanocrystal-based films showing bright photoluminescence can be fabricated via a new centrifugal casting process, directly from a crude synthesis solution. The casting process enables simultaneous purification and film fabrication, and overcomes the problems of aggregation and segregation arising from the application of prior film-forming techniques to the deposition of these new materials.

In addition, centrifugally cast films of $CsPbBr_3$ nanocrystals exhibited outstanding PLQY. This work represents the first report of highly luminescent films composed of perovskite quantum dots that do not require the inclusion of insulating matrix materials that militate against charge transport.

■ ASSOCIATED CONTENT

Supporting Information

The Supporting Information is available free of charge on the ACS Publications website at DOI: 10.1021/acsami.5b09084.

Experimental section; UV−vis and PL spectra; additional TEM, SEM, and AFM images (PDF)

■ AUTHOR INFORMATION

Corresponding Author

*E-mail: ted.sargent@utoronto.ca.

Present Address

#P.K.: Materials Science and Engineering, Faculty of Science, Mahidol University, 272 Rama 6 Rd., Ratchathewi District, Bangkok, 10400, Thailand.

Notes

The authors declare no competing financial interest.

■ ACKNOWLEDGMENTS

This publication is based in part on work supported by Award KUS-11-009-21, made by King Abdullah University of Science and Technology (KAUST), by the Ontario Research Fund Research Excellence Program, and by the Natural Sciences and Engineering Research Council (NSERC) of Canada. E.Y. acknowledges support from Sao Paulo State Research Foundation-Research Internships Abroad (FAPESP-BEPE) (2014/18327-9) fellowship. The authors thank E. Palmiano, R. Wolowiec, and D. Kopilovic for their technical help over the course of this study. We thank the Centre for Microfluidic Systems in Chemistry and Biology (Toronto, Ontario) for the use of an atomic force microscope.

■ REFERENCES

(1) Burschka, J.; Pellet, N.; Moon, S.-J.; Humphry-Baker, R.; Gao, P.; Nazeeruddin, M. K.; Grätzel, M. Sequential Deposition as a Route to High-Performance Perovskite-Sensitized Solar Cells. *Nature* **2013**, *499*, 316−319.

(2) Lee, M. M.; Teuscher, J.; Miyasaka, T.; Murakami, T. N.; Snaith, H. J. Efficient Hybrid Solar Cells Based on Meso-Superstructured Organometal Halide Perovskites. *Science* **2012**, *338*, 643−647.

(3) Jeon, N. J.; Noh, J. H.; Yang, W. S.; Kim, Y. C.; Ryu, S.; Seo, J.; Seok, S. I. Compositional Engineering of Perovskite Materials for High-Performance Solar Cells. *Nature* **2015**, *517*, 476−481.

(4) Yang, W. S.; Noh, J. H.; Jeon, N. J.; Kim, Y. C.; Ryu, S.; Seo, J.; Seok, S. I. High-Performance Photovoltaic Perovskite Layers Fabricated through Intramolecular Exchange. *Science* **2015**, *348*, 1234−1237.

(5) Tan, Z.-K.; Moghaddam, R. S.; Lai, M. L.; Docampo, P.; Higler, R.; Deschler, F.; Price, M.; Sadhanala, A.; Pazos, L. M.; Credgington, D.; Hanusch, F.; Bein, T.; Snaith, H. J.; Friend, R. H. Bright Light-Emitting Diodes Based on Organometal Halide Perovskite. *Nat. Nanotechnol.* **2014**, *9*, 687−691.

(6) Hoye, R. L. Z.; Chua, M. R.; Musselman, K. P.; Li, G.; Lai, M.-L.; Tan, Z.-K.; Greenham, N. C.; MacManus-Driscoll, J. L.; Friend, R. H.; Credgington, D. Enhanced Performance in Fluorene-Free Organometal Halide Perovskite Light-Emitting Diodes Using Tunable, Low Electron Affinity Oxide Electron Injectors. *Adv. Mater.* **2015**, *27*, 1414−1419.

(7) Wang, J.; Wang, N.; Jin, Y.; Si, J.; Tan, Z.-K.; Du, H.; Cheng, L.; Dai, X.; Bai, S.; He, H.; Ye, Z.; Lai, M. L.; Friend, R. H.; Huang, W. Interfacial Control toward Efficient and Low-Voltage Perovskite Light-Emitting Diodes. *Adv. Mater.* **2015**, *27*, 2311−2316.

(8) Deschler, F.; Price, M.; Pathak, S.; Klintberg, L. E.; Jarausch, D.-D.; Higler, R.; Hüttner, S.; Leijtens, T.; Stranks, S. D.; Snaith, H. J.; Atatüre, M.; Phillips, R. T.; Friend, R. H. High Photoluminescence Efficiency and Optically Pumped Lasing in Solution-Processed Mixed Halide Perovskite Semiconductors. *J. Phys. Chem. Lett.* **2014**, *5*, 1421−1426.

(9) Sutherland, B. R.; Hoogland, S.; Adachi, M. M.; Wong, C. T. O.; Sargent, E. H. Conformal Organohalide Perovskites Enable Lasing on Spherical Resonators. *ACS Nano* **2014**, *8*, 10947−10952.

(10) DInnocenzo, V.; Kandada, A. R. S.; Bastiani, M. D.; Gandini, M.; Petrozza, A. Tuning the Light Emission Properties by Band Gap Engineering in Hybrid Lead Halide Perovskite. *J. Am. Chem. Soc.* **2014**, *136*, 17730−17733.

(11) Noel, N. K.; Abate, A.; Stranks, S. D.; Parrott, E. S.; Burlakov, V. M.; Goriely, A.; Snaith, H. J. Enhanced Photoluminescence and Solar Cell Performance *via* Lewis Base Passivation of Organic-Inorganic Lead Halide Perovskites. *ACS Nano* **2014**, *8*, 9815−9821.

(12) Schmidt, L. C.; Pertegás, A.; González-Carrero, S.; Malinkiewicz, O.; Agouram, S.; Espallargas, G. M.; Bolink, H. J.; Galian, R. E.; Pérez-Prieto, J. Nontemplate Synthesis of $CH_3NH_3PbBr_3$ Perovskite Nanoparticles. *J. Am. Chem. Soc.* **2014**, *136*, 850−853.

(13) Protesescu, L.; Yakunin, S.; Bodnarchuk, M. I.; Krieg, F.; Caputo, R.; Hendon, C. H.; Yang, R. X.; Walsh, A.; Kovalenko, M. V. Nanocrystals of Cesium Lead Halide Perovskites ($CsPbX_3$, X = Cl, Br, and I): Novel Optoelectronic Materials Showing Bright Emission with Wide Color Gamut. *Nano Lett.* **2015**, *15*, 3692−3696.

(14) Nedelcu, G.; Protesescu, L.; Yakunin, S.; Bodnarchuk, M. I.; Grotevent, M. J.; Kovalenko, M. V. Fast Anion-Exchange in Highly Luminescent Nanocrystals of Cesium Lead Halide Perovskites ($CsPbX_3$, X= Cl, Br, I). *Nano Lett.* **2015**, *15*, 5635−5640.

(15) Zhang, F.; Zhong, H.; Chen, C.; Wu, X.-G.; Hu, X.; Huang, H.; Han, J.; Zou, B.; Dong, Y. Brightly Luminescent and Color-Tunable Colloidal $CH_3NH_3PbX_3$ (X = Br, I, Cl) Quantum Dots: Potential Alternatives for Display Technology. *ACS Nano* **2015**, *9*, 4533−4542.

(16) Akkerman, Q. A.; DInnocenzo, V.; Accornero, S.; Scarpellini, A.; Petrozza, A.; Prato, M.; Manna, L. Tuning the Optical Properties of Cesium Lead Halide Perovskite Nanocrystals by Anion Exchange Reactions. *J. Am. Chem. Soc.* **2015**, *137*, 10276−10281.

DOI: 10.1021/acsami.5b09084
ACS Appl. Mater. Interfaces XXXX, XXX, XXX−XXX

(17) Zhang, D.; Eaton, S. W.; Yu, Y.; Dou, L.; Yang, P. Solution-Phase Synthesis of Cesium Lead Halide Perovskite Nanowires. *J. Am. Chem. Soc.* **2015**, *137*, 9230−9233.
(18) Huang, H.; Susha, A. S.; Kershaw, S. V.; Hung, T. F.; Rogach, A. L. Control of Emission Color of High Quantum Yield $CH_3NH_3PbBr_3$ Perovskite Quantum Dots by Precipitation Temperature. *Adv. Mater.* **2015**, *2*, DOI: 10.1002/advs.201500194
(19) Park, J.; An, K.; Hwang, Y.; Park, J.-G.; Noh, H.-J.; Kim, J.-Y; Park, J.-H.; Hwang, N.-M.; Hyeon, T. Ultra-Large-Scale Syntheses of Monodisperse Nanocrystals. *Nat. Mater.* **2004**, *3*, 891−895.
(20) Ko, Y.; Baek, H.; Kim, Y.; Yoon, M.; Cho, J. Hydrophobic Nanoparticle-Based Nanocomposite Films Using *In Situ* Ligand Exchange Layer-by-Layer Assembly and Their Nonvolatile Memory Applications. *ACS Nano* **2013**, *7*, 143−153.
(21) Zhao, Y.; Zhu, K. Charge Transport and Recombination in Perovskite $(CH_3NH_3)PbI_3$ Sensitized TiO_2 Solar Cells. *J. Phys. Chem. Lett.* **2013**, *4*, 2880−2884.
(22) Samuels, M. L.; Schuh, A. E. Some Recent Developments in Centrifugal Casting. *Foundry* **1951**, 84.
(23) Biesheuvel, P. M.; Nijmeijer, A.; Kerkwijk, B.; Verweij, H. Rapid Manufacturing of Microlaminates by Centrifugal Injection Casting. *Adv. Eng. Mater.* **2000**, *2*, 507−510.
(24) Melcher, R.; Cromme, P.; Scheffler, M.; Greil, P. Centrifugal Casting of Thin-Walled Ceramic Tubes from Preceramic Polymers. *J. Am. Ceram. Soc.* **2003**, *86*, 1211−1213.
(25) Rao, P.; Iwasa, M.; Tanaka, T.; Kondoh, I. Centrifugal Casting of Al_2O_3-15 wt.%ZrO_2 Ceramic Composites. *Ceram. Int.* **2003**, *29*, 209−212.
(26) Kim, J. Y.; Adinolfi, V.; Sutherland, B. R.; Voznyy, O.; Kwon, S. J.; Kim, T. W.; Kim, J.; Ihee, H.; Kemp, K.; Adachi, M.; Yuan, M.; Kramer, I.; Zhitomirsky, D.; Hoogland, S.; Sargent, E. H. Single-Step Fabrication of Quantum Funnels *via* Centrifugal Colloidal Casting of Nanoparticle Films. *Nat. Commun.* **2015**, *6*, 7772.
(27) Stoumpos, C. C.; Malliakas, C. D.; Peters, J. A.; Liu, Z.; Sebastian, M.; Im, J.; Chasapis, T. C.; Wibowo, A. C.; Chung, D. Y.; Freeman, A. J.; Wessels, B. W.; Kanatzidis, M. G. Crystal Growth of the Perovskite Semiconductor $CsPbBr_3$: A New Material for High-Energy Radiation Detection. *Cryst. Growth Des.* **2013**, *13*, 2722−2727.
(28) Smith, I. C.; Hoke, E. T.; Solis-Ibarra, D.; McGehee, M. D.; Karunadasa, H. I. A Layered Hybrid Perovskite Solar-Cell Absorber with Enhanced Moisture Stability. *Angew. Chem.* **2014**, *126*, 11414−11417.
(29) Chang, T.-W. F.; Maria, A.; Cyr, P. W.; Sukhovatkin, V.; Levina, L.; Sargent, E. H. High Near-Infrared Photoluminescence Quantum Efficiency from PbS Nanocrystals in Polymer Films. *Synth. Met.* **2005**, *148*, 257−261.
(30) Comin, R.; Walters, G.; Thibau, E. S.; Voznyy, O.; Lu, Z.-H.; Sargent, E. H. Structural, Optical, and Electronic Studies of Wide-Bandgap Lead Halide Perovskites. *J. Mater. Chem. C* **2015**, *3*, 8839−8843.

DOI: 10.1021/acsami.5b09084
ACS Appl. Mater. Interfaces XXXX, XXX, XXX−XXX